

# Alkyl Chain Length Defines 2D Architecture of Salophen Complexes on Liquid–Graphite Interface

Minna T. Räisänen,<sup>[a]</sup> Florian Mögele,<sup>[b]</sup> Santeri Feodorow,<sup>[a]</sup> Bernhard Rieger,<sup>[b]</sup>  
Ulrich Ziener,<sup>[c]</sup> Markku Leskelä,<sup>[a]</sup> and Timo Repo<sup>\*[a]</sup>

**Keywords:** Metal-containing monolayers / Nanopatterning / Scanning tunnelling microscopy (STM) / Self-assembly

A series of Cu<sup>II</sup>, Ni<sup>II</sup> and Co<sup>II</sup> salophen [salophen = *N,N'*-(*o*-phenylene)bis(salicylideneimine)] complexes were prepared, and their two-dimensional (2D) assemblies on a liquid–graphite interface were studied by scanning tunnelling microscopy (STM). Depending on their varying alkyl chain lengths (C<sub>8</sub>, C<sub>10</sub> or C<sub>12</sub>), two different new adlayers, parallelogram and honeycomb, were recorded. According to STM data, the driving force for these assemblies is a subtle interplay between a maximum amount of attractive van der Waals

interaction of the alkyl chains and weak hydrogen bonding of the phenoxy moieties. Thus, the alkyl chain length defines the favoured 2D structure for each metal complex. As shown here, the self-assembled monolayers of the salophen complexes studied provide an attractive approach to varying the surface architecture.

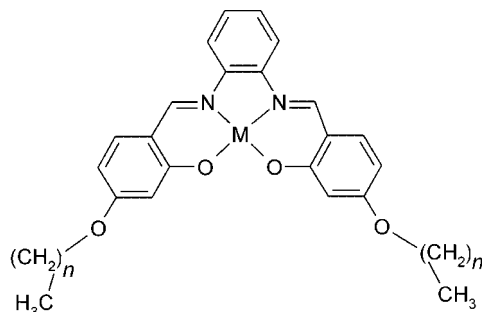
(© Wiley-VCH Verlag GmbH & Co. KGaA, 69451 Weinheim, Germany, 2007)

## Introduction

The formation of self-assembled monolayers (SAMs) is a useful methodology for the preparation of surfaces with well-defined composition, structure and thickness.<sup>[1]</sup> SAMs have found use in chemical sensors,<sup>[2]</sup> electrochemistry,<sup>[3]</sup> catalysis,<sup>[4]</sup> corrosion protection,<sup>[5]</sup> lubrication,<sup>[6]</sup> adhesion<sup>[7]</sup> and wetting.<sup>[7,8]</sup> Lately, SAMs of metal complexes on highly oriented pyrolytic graphite (HOPG) have captured significant interest,<sup>[9]</sup> as they provide a platform for the highly ordered metal-decorated surfaces required in such uses as functional nano devices and data storage.<sup>[10]</sup> For example, the controlled 2D or 3D assembly of [2 × 2] M<sup>II</sup> grid-type complexes of Co<sup>[11]</sup> and Fe<sup>[12]</sup> is important, as these complexes have many technologically interesting properties.<sup>[13]</sup> Furthermore, redox-active Ru<sup>II</sup> and Pt<sup>II</sup> Fréchet dendrons have been assembled on HOPG.<sup>[14]</sup> In addition to assemblies on HOPG, several metal–organic coordination networks have been studied on single crystalline Cu, Au and Ag surfaces for the preparation of functional nanomaterials.<sup>[15]</sup>

For application purposes, the highly oriented SAMs must be kinetically and thermodynamically stable in the long run

in order to maintain their desired function. Intermolecular van der Waals interactions – especially those of long alkyl chains – as well as hydrogen bonding and adsorbate–substrate interactions within the 2D arrays provide strong driving forces for the formation of highly ordered surface structures. Long alkyl chains play a considerable role in the mutual recognition and stabilisation of the patterns formed and act as easily variable spacers.<sup>[9d,9f]</sup> In this context, we report herein a study of 2D assemblies for a series of Co<sup>II</sup>, Cu<sup>II</sup> and Ni<sup>II</sup> salophen complexes (1–9) on a liquid–graphite interface (Figure 1). Depending on their varying alkyl chain lengths (C<sub>8</sub>, C<sub>10</sub> or C<sub>12</sub>), the salophen complexes formed two different new adlayers on HOPG.



1: M = Cu<sup>2+</sup>, *n* = 11; 2: M = Cu<sup>2+</sup>, *n* = 9; 3: M = Cu<sup>2+</sup>, *n* = 7;  
4: M = Ni<sup>2+</sup>, *n* = 11; 5: M = Ni<sup>2+</sup>, *n* = 9; 6: M = Ni<sup>2+</sup>, *n* = 7;  
7: 1: M = Co<sup>2+</sup>, *n* = 11; 8: 1: M = Co<sup>2+</sup>, *n* = 9; 9: M = Co<sup>2+</sup>, *n* = 7.

Figure 1. Schematic structures of salophen complexes 1–9.

[a] Laboratory of Inorganic Chemistry, Department of Chemistry, University of Helsinki  
P.O. Box 55, 00014 University of Helsinki, Finland  
Fax: +358-9-191-50198  
E-Mail: timo.repo@helsinki.fi

[b] Department of Materials and Catalysis, University of Ulm  
Albert-Einstein-Allee 11, 89081 Ulm, Germany

[c] Department of Organic Chemistry III, Macromolecular Chemistry, University of Ulm  
Albert-Einstein-Allee 11, 89081 Ulm, Germany

Supporting information for this article is available on the WWW under <http://www.eurjic.org> or from the author.

## Results and Discussion

Salophen ligand precursors with varying alkyl chain lengths and their  $\text{Co}^{\text{II}}$ ,  $\text{Cu}^{\text{II}}$  and  $\text{Ni}^{\text{II}}$  complexes (**1–9**) were prepared by standard synthetic procedures (see Exp. Sect.). The self-assembled monolayers of **1–9** were measured at room temperature in saturated 1,2,4-trichlorobenzene (TCB) solutions by STM at the liquid–solid interface on HOPG.<sup>[16]</sup> The images were measured in a constant-current mode, and the aromatic parts of the molecules appear brighter than the alkyl chains because of their higher electron density. In addition to the SAMs of the metal complexes, those of the uncomplexed salophen ligand **E** with  $\text{C}_{12}$  alkyl chains were imaged. The surface structure formed was of lamellar type with interdigitating alkyl chains (Figure 2) and clearly distinct from those of the complexes deposited on HOPG from the same solvent (TCB). In the case of ligands with shorter alkyl chains ( $\text{C}_{10}$  and  $\text{C}_8$ ), no images

were obtained under the same conditions as those used for the metal complexes.<sup>[16]</sup>

So far the most common 2D structure reported for metal complexes on HOPG is a highly ordered lamellar structure similar to that measured here for the uncomplexed salophen ligand.<sup>[9a,9b,9c–9g]</sup> Therefore, it was quite unexpected that all salophen complexes bearing short ( $\text{C}_{10}$  or  $\text{C}_8$ ) alkyl chains would assemble on the HOPG surface by forming an array of almost distinct parallelograms rather than striped lamellar structures (Figure 3). The attribution of the bright features to the aromatic parts of the molecule leads to a proposed model where each parallelogram consists of four salophen complexes. Detailed analysis of the 2D structure revealed its novelty.

The interatomic distances between neighbouring molecules in the structure can be estimated from the model coinciding with the high-resolution STM pattern. As shown

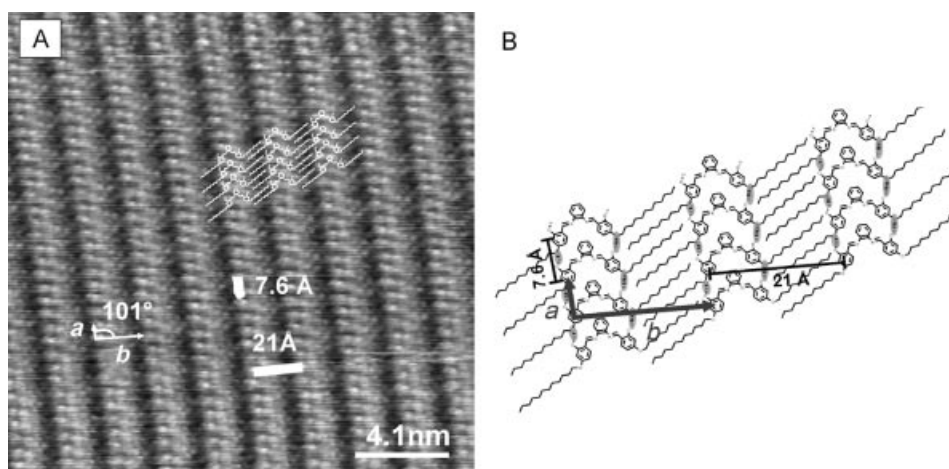


Figure 2. The STM image (A) and the proposed molecular model (B) for *N,N'*-(*o*-phenylene)bis(4-decyloxysalicylideneimine) (**E**) on HOPG. The image was obtained from saturated 1,2,4-trichlorobenzene solution. Image area:  $203 \text{ \AA} \times 203 \text{ \AA}$ ;  $U_{\text{set}} = -259 \text{ mV}$ ;  $I_{\text{set}} = 18.2 \text{ pA}$ . Unit cell dimensions:  $a = 7.6 \pm 0.2 \text{ \AA}$ ;  $b = 21.0 \pm 0.2 \text{ \AA}$ ; angle  $101 \pm 2^\circ$ . The hydrogen bonding of molecules is shown by the dotted lines and the grey overlay.

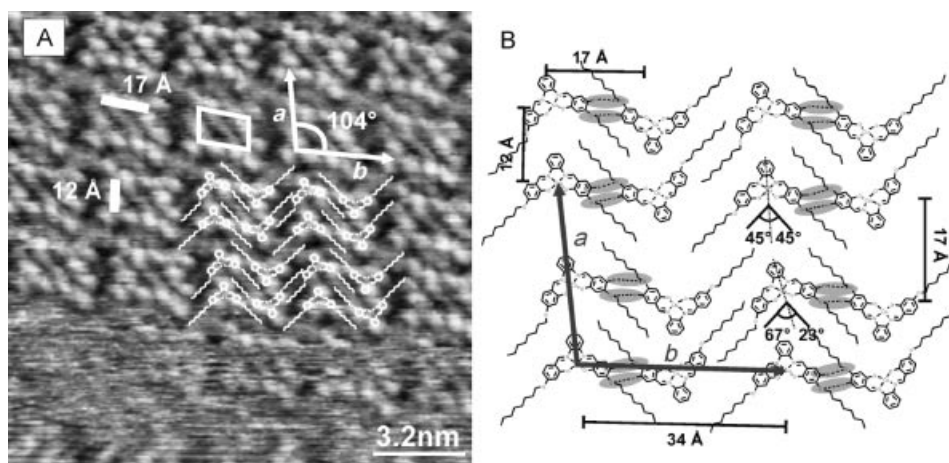


Figure 3. The high-resolution STM image (A) and the proposed molecular model (B) for complex **3** at the liquid–HOPG interface. Image area:  $161 \text{ \AA} \times 161 \text{ \AA}$ ;  $U_{\text{set}} = -630 \text{ mV}$ ;  $I_{\text{set}} = 29.3 \text{ pA}$ . Unit cell dimensions:  $a = 28.5 \pm 0.2 \text{ \AA}$ ;  $b = 34.0 \pm 0.2 \text{ \AA}$ ; angle  $104 \pm 2^\circ$ . The hydrogen bonding in a parallelogram is shown by the dotted lines and the grey overlay.

here for **3**, intermolecular metal–metal distances within a parallelogram alternate between  $12.0 \pm 0.2$  Å (*a* axis) and  $17.0 \pm 0.2$  Å (*b* axis), while the shortest metal–metal distances between the parallelograms, regardless of the axis, are constant at a value of  $17.0 \pm 0.2$  Å (Figure 3). The metal–metal distances along the *b* axis can be considered as the distances between the lamellae. This structure consists of two different, alternating lamellae that differ from each other by the relative orientation of the salophen complexes. In the proposed structural model, every second complex within a lamella is also twisted by  $18^\circ$  with respect to the preceding molecule, which further distorts the classical lamellar structure. If a parallelogram is considered to be a unit, it can be seen that the periodicity of this structure is 34 Å along the *b* axis and 29 Å along the *a* axis. Specifically, the differing orientation of the molecules and the resulting loss of symmetry within a lamella distinguish this parallelogram-like structure from the traditional lamellar structure. A parallelogram-like structure similar to that of **3** was also obtained for Ni and Co complexes **5**, **6**, **8** and **9** bearing C<sub>10</sub> and C<sub>8</sub> alkyl chains (see Supporting Information). As illustrated in Table 1, the variation of the alkyl chain length and central metal ion has an observable influence on the geometry of the 2D structure obtained. For example, the Co complexes **8** (C<sub>10</sub>) and **9** (C<sub>8</sub>) have a rather constant *b* axis, whereas the change in the alkyl chain length has a substantial influence on the *a* axis. Similarly, the difference in the *b* axis is only ca. 1 Å in Ni complexes **5** (C<sub>10</sub>) and **6** (C<sub>8</sub>), whereas the *a* axis is longer by ca. 3 Å in the complex with the longer alkyl chain. Although the image resolutions of **5**, **6**, **8** and **9** do not facilitate the interpretation of the 2D fine structures, it is clear that the length of the alkyl chain and the nature of the metal ion play an interactive role in the formation of these structures.

Table 1. Unit cell dimensions of salophen complexes **3**, **5**, **6**, **8** and **9** with parallelogram-like 2D structures.

Complex	Unit cell dimensions		
	<i>a</i> [Å]	<i>b</i> [Å]	Angle [°]
CuC <sub>8</sub> ( <b>3</b> )	$28.5 \pm 0.2$	$34.0 \pm 0.2$	$104 \pm 2$
NiC <sub>10</sub> ( <b>5</b> )	$28.0 \pm 0.2$	$28.0 \pm 0.2$	$90 \pm 2$
NiC <sub>8</sub> ( <b>6</b> )	$25.0 \pm 0.2$	$27.0 \pm 0.2$	$95 \pm 2$
CoC <sub>10</sub> ( <b>8</b> )	$28.0 \pm 0.2$	$33.5 \pm 0.2$	$92 \pm 2$
CoC <sub>8</sub> ( <b>9</b> )	$22.0 \pm 0.2$	$34.0 \pm 0.2$	$100 \pm 2$

The measured lamellar periodicities suggest that the alkyl chains of neighbouring lamellae interdigitate. The darker regions in Figure 3A exhibit a striped pattern that approximates the distance between the alkyl chains, which averages  $5.0 \pm 0.2$  Å. This is a rather typical value for close-packed alkyl chains in van der Waals contact.<sup>[17]</sup> The alkyl chains need to adjust themselves to the adjacent molecule; this results in different angles ( $23^\circ$ ,  $45^\circ$  or  $67^\circ$ ) between the alkyl chains and the bisectors of the molecules. As a result of the distorted lamellar structure, the interdigitation of the alkyl chains also varies in the assembly. In a parallelogram, one alkyl chain of a complex in the upper left-hand corner and one of a complex in the lower right-hand corner fully interdigitate with alkyl chains of complexes in two neighbouring

parallelograms, and this particular interaction actually joins the individual parallelograms together to form a continuous pattern. Further on, the remaining alkyl chains of these complexes fully interdigitate with each other. Interdigitation of the alkyl chains of complexes in the lower left-hand and upper right-hand corners, even to a relatively low degree, with the molecules of neighbouring parallelograms provides additional stabilisation for the assembly.

In addition to the above-described van der Waals interactions, the parallelogram-like structure appears to be further stabilised by intermolecular C<sub>Ar</sub>H...O<sub>alkoxy</sub> hydrogen bonding. Inside a given parallelogram are two pairs of hydrogen-bond-coupled salophen complexes (Figure 3). The observed hydrogen bond lengths of ca.  $2.7 \pm 0.2$  Å fall within the range of weak hydrogen bonds.<sup>[18]</sup> According to the molecular symmetry, these hydrogen-bonded couples inside each parallelogram are identical. In this respect, the 2D assembly can also be seen as an arrangement of those hydrogen-bonded couples rather than that of individual salophen complexes. It is noteworthy that there is no interparallelogram hydrogen bonding. We assume that the hydrogen bonding is essential in stabilising the 2D structure, which represents the global energetic minimum gained by a compromise between the hydrogen bonding and the maximum amount of van der Waals contacts. Both of these intermolecular interactions are known to be important structural parameters in 2D assemblies,<sup>[9a,19,20]</sup> and the influence of alkyl chain length on the 2D structure was described previously for the co-adsorption of trimesic acid with even- and odd-numbered alcohols on HOPG.<sup>[20]</sup>

In this series of salophen complexes, an increase in the alkyl chain length from C<sub>10</sub> to C<sub>12</sub> leads exclusively to a new, honeycomb-type network pattern consisting of hexagons with six molecules.<sup>[21]</sup> A structural model in which each molecule has its three nearest neighbours within a range of  $12.0 \pm 0.2$  Å to  $15.0 \pm 0.2$  Å is proposed (Figure 4). In this assembly, the alkyl chains of each molecule are parallel to the bisector of the salophen complex and interdigitate perfectly with those of the opposite molecule within each hexagon. Thus, in the honeycomb assembly, the alkyl chains only form van der Waals contacts inside the hexagons, whereas in the classical lamellar assembly as well as in the parallelogram-like one described above, they form a continuous network throughout the 2D structures. Instead, here the hydrogen-bonding network continues throughout the structure, and every complex has two intermolecular C<sub>Ar</sub>H...O<sub>alkoxy</sub> hydrogen bonds at an approximate distance of  $2.6 \pm 0.2$  Å. This distance was estimated by applying typical geometric parameters to the structural model in Figure 4B. Apparently, both van der Waals contacts and hydrogen bonding are needed to stabilise this assembly.

The substantial differences in the 2D packings of the salophen-C<sub>12</sub> ligand **E** and its Co<sup>II</sup> complex **7** can be explained by the effect of the Co<sup>II</sup> ion on the ligand geometry upon complex formation. When the salophen ligand coordinates to the Co<sup>II</sup> ion, both hydroxy groups are forced towards the metal ion, and the complex acquires an overall C<sub>2</sub> symmetry. On the contrary, in the free ligand **E**, the OH groups



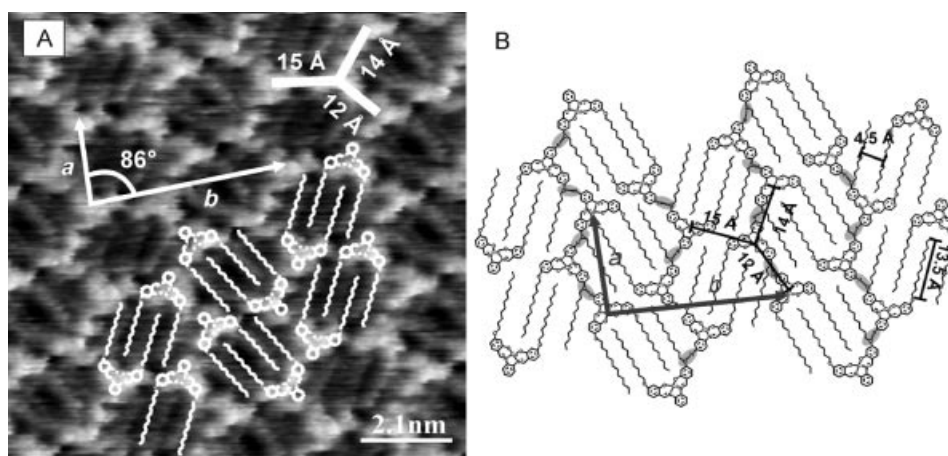


Figure 4. The high-resolution STM image (A) and the proposed molecular model (B) for complex 7. Image area:  $104 \text{ \AA} \times 104 \text{ \AA}$ ;  $U_{\text{set}} = -180 \text{ mV}$ ;  $I_{\text{set}} = 12.8 \text{ pA}$ . Unit cell dimensions:  $a = 19.5 \pm 0.2 \text{ \AA}$ ;  $b = 46.0 \pm 0.2 \text{ \AA}$ ; angle =  $86 \pm 2^\circ$ . The hydrogen bonding in a honeycomb is shown by the dotted lines and the grey overlay.

can be located independently either inside or outside the ligand cavity as a result of rotation. In the 2D structure of **E** (Figure 2), both hydroxy groups point outwards, forming hydrogen bonds with the adjacent molecule.

Clear differences can be noted in the stabilisation of the 2D parallelogram-like and honeycomb structures. In the parallelogram-like structure the van der Waals forces are reduced as a result of the twisted orientation of every second complex in a lamella, but this reduced stability is compensated for by hydrogen bonds inside the parallelogram. The van der Waals interactions network the structure. In the honeycomb assembly, alkyl chains of an individual complex fully interdigitate with alkyl chains of another complex, but further networking is prohibited by the surrounding ligand frameworks. Hydrogen bonds form the required network and are essential in stabilising the honeycomb structure. Apparently, by tuning the alkyl chain length in salophen complexes, the balance between van der Waals and hydrogen bonding interactions can be controlled. As a consequence, the 2D assembly of the complexes changes. These findings are summarised in Table 2 to illustrate the interactive effects of van der Waals interactions, i.e. the alkyl chain length, and hydrogen bonding on the 2D morphology of the SAMs. Furthermore, metal ions have clear effects on the 2D assemblies, as shown by the formation of a lamellar structure by the uncomplexed  $\text{C}_{12}$  ligand (Figure 2).

Table 2. The van der Waals interactions and number of hydrogen bonds in parallelogram-like and honeycomb structures.

2D structure	van der Waals interactions	H bonds per molecule	Networking by
Parallelogram-like: $\text{CoC}_8$ , $\text{CuC}_8$ , $\text{NiC}_8$ , $\text{CoC}_{10}$ , $\text{NiC}_{10}$	Alkyl chains of every second molecule are fully interdigitating.	2	van der Waals interactions
Honeycomb: $\text{CoC}_{12}$ , $\text{NiC}_{12}$	Alkyl chains of each molecule are fully interdigitating.	2	Hydrogen bonds

Regardless of the surface architecture and hence different metal ion patterning on the surface, both structures exhibit rather similar metal ion densities. The parallelogram-like assembly has a packing where the average metal ion coverage is ca.  $0.52/\text{nm}^2$ , whereas in the honeycomb structure the value is ca.  $0.48/\text{nm}^2$  (values are estimated from a  $5 \text{ nm} \times 5 \text{ nm}$  area).

## Conclusions

STM studies of salophen complexes on liquid-graphite interfaces revealed new parallelogram-like and honeycomb structures. As demonstrated here, the alkyl chain length can have a significant influence in determining the assembly of the salophen complexes. Complexes bearing  $\text{C}_8$  or  $\text{C}_{10}$  alkyl chains assemble in the parallelogram-like 2D structure, while those with  $\text{C}_{12}$  alkyl chains form the honeycomb assembly. The driving force for these new assemblies is a subtle interplay between a maximum amount of attractive van der Waals interactions of the alkyl chains and weak hydrogen bonding. Because of the ease of the methodology of SAM formation and the straightforward synthesis of salophen complexes, the SAMs of these compounds provide an attractive approach for the fine tuning of the surface architecture.

## Experimental Section

**General Methods and Materials:**  $^1\text{H}$  NMR spectra were recorded with a Varian Gemini 200 apparatus, and IR spectra were taken with a PerkinElmer Spectrum One.  $\text{EI}^+$  and HRMS ( $\text{ESI}^+$  TOF) mass spectra were recorded with a JEOL JMS-SX 102 (ionising voltage  $70 \text{ eV}$ ) and with a Bruker micrOTOF mass spectrometer, respectively. Elemental analyses were performed with an EA 1110 CHNS-O CE instrument. For STM measurements, a low-current RHK scanning tunnelling microscope was used, which was operated in a constant-current mode under ambient conditions. STM tips were mechanically sharpened from Pt/Ir (80:20) wire, and HOPG was used as a substrate for the adlayers. The compounds

were dissolved in 1,2,4-trichlorobenzene, and a droplet of the saturated solution was placed on freshly cleaved HOPG. All chemicals required for complex synthesis were purchased from Aldrich and used as received. STM images were processed with WSxM<sup>®</sup>.

**Ligands:** 4-dodecyloxy-2-hydroxybenzaldehyde (**A**), 4-decyloxy-2-hydroxybenzaldehyde (**B**) and 4-octyloxy-2-hydroxybenzaldehyde (**C**) were prepared with moderate yields according to a procedure by Binnemans et al.<sup>[22]</sup>

***N,N'*-(*o*-Phenylene)bis(4-dodecyloxysalicylideneimine) (**D**):** (*o*-Phenylene)diamine (1.412 g, 13 mmol) in MeOH (20 mL) was added to compound **A** (8.005 g, 26 mmol) dissolved in *n*-hexane (20 mL). A yellow colour immediately appeared, and the solution was stirred at room temperature for 18 h. The viscous product obtained was stirred in MeOH for 2 h, and the yellow powder that was formed was filtered, washed with MeOH and finally dried in vacuo (isolated yield 7.156 g, 40%). Analytical data for C<sub>44</sub>H<sub>64</sub>N<sub>2</sub>O<sub>4</sub>: <sup>1</sup>H NMR (200 MHz, CDCl<sub>3</sub>, 25 °C, TMS): δ = 0.94 (t, <sup>3</sup>J<sub>H,H</sub> = 7.0 Hz, 6 H, CH<sub>3</sub>), 1.32 (s, 36 H, CH<sub>2</sub>), 1.76–1.90 (m, 4 H, CH<sub>2</sub>), 4.03 (t, <sup>3</sup>J<sub>H,H</sub> = 6.7 Hz, 4 H, OCH<sub>2</sub>), 6.51 (dd, *J*<sub>H,H</sub> = 2.4 Hz, <sup>3</sup>J<sub>H,H</sub> = 8.5 Hz, 2 H, Ar-H), 6.58 (d, <sup>3</sup>J<sub>H,H</sub> = 2.2 Hz, 2 H, Ar-H), 7.23–7.36 (m, 6 H, Ar-H), 8.58 (s, 2 H, HC=N) ppm. IR: ν̄ = 1609 (C=N), 1583 (C=C), 1246 (C–O) cm<sup>−1</sup>. HRMS (ESI-TOF): calcd. for [M + H]<sup>+</sup> 685.4939; found 685.4938; error 0.08 ppm.

Salophen ligands **E** and **F** were synthesised in the same manner as ligand **D**.

***N,N'*-(*o*-Phenylene)bis(4-decyloxysalicylideneimine) (**E**):** Yellow powder (isolated yield 31%). Analytical data for C<sub>40</sub>H<sub>56</sub>N<sub>2</sub>O<sub>4</sub>: <sup>1</sup>H NMR (200 MHz, CDCl<sub>3</sub>, 25 °C, TMS): δ = 0.89 (t, <sup>3</sup>J<sub>H,H</sub> = 6.9 Hz, 6 H, CH<sub>3</sub>), 1.28 (s, 28 H, CH<sub>2</sub>), 1.71–1.85 (m, 4 H, CH<sub>2</sub>), 3.98 (t, <sup>3</sup>J<sub>H,H</sub> = 6.7 Hz, 4 H, OCH<sub>2</sub>), 6.38 (dd, *J*<sub>H,H</sub> = 2.4 Hz, <sup>3</sup>J<sub>H,H</sub> = 8.9 Hz, 2 H, Ar-H), 6.45 (d, <sup>3</sup>J<sub>H,H</sub> = 2.3 Hz, 2 H, Ar-H), 7.18–7.31 (m, 6 H, Ar-H), 8.53 (s, 2 H, HC=N) ppm. IR: ν̄ = 1608 (C=N), 1582 (C=C), 1240 (C–O) cm<sup>−1</sup>. HRMS (ESI-TOF): calcd. for [M + H]<sup>+</sup> 629.4313; found 629.4330; error −2.66 ppm.

***N,N'*-(*o*-Phenylene)bis(4-octyloxysalicylideneimine) (**F**):** Yellow powder (isolated yield 56%). Analytical data for C<sub>36</sub>H<sub>48</sub>N<sub>2</sub>O<sub>4</sub>: <sup>1</sup>H NMR (200 MHz, CDCl<sub>3</sub>, 25 °C, TMS): δ = 0.89 (t, <sup>3</sup>J<sub>H,H</sub> = 6.9 Hz, 6 H, CH<sub>3</sub>), 1.30 (s, 20 H, CH<sub>2</sub>), 1.72–1.85 (m, 4 H, CH<sub>2</sub>), 3.98 (t, <sup>3</sup>J<sub>H,H</sub> = 6.5 Hz, 4 H, OCH<sub>2</sub>), 6.46 (dd, *J*<sub>H,H</sub> = 2.4 Hz, <sup>3</sup>J<sub>H,H</sub> = 8.4 Hz, 2 H, Ar-H), 6.53 (d, <sup>3</sup>J<sub>H,H</sub> = 2.0 Hz, 2 H, Ar-H), 7.18–7.31 (m, 6 H, Ar-H), 8.53 (s, 2 H, CH=N) ppm. IR: ν̄ = 1608 (C=N), 1582 (C=C), 1240 (C–O) cm<sup>−1</sup>. HRMS (ESI-TOF): calcd. for [M + H]<sup>+</sup> 573.3687; found 573.3701; error −2.44 ppm.

**Complexes:** Cobalt complexes were prepared under an Ar atmosphere by using standard Schlenk techniques. Copper and nickel complexes were synthesised under ambient conditions. Dry solvents were used in the preparation of cobalt complexes. Crude products of nickel and copper complexes were washed with MeOH and *n*-hexane, and they were finally recrystallised from CHCl<sub>3</sub> or CH<sub>2</sub>Cl<sub>2</sub>. Crude products of the cobalt complexes were washed with MeOH.

***N,N'*-(*o*-Phenylene)bis(4-dodecyloxysalicylideneiminato)copper(II) (**1**):** A warmed solution of Cu(OOCCH<sub>3</sub>)<sub>2</sub> (0.133 g, 0.73 mmol) in MeOH (40 mL) was added to a solution of **D** (0.500 g, 0.74 mmol) in CH<sub>2</sub>Cl<sub>2</sub> (10 mL). A brown suspension immediately formed and was stirred at room temperature for 20 h. A green precipitate was filtered and washed with MeOH and *n*-hexane. Finally the crude product was recrystallised from CH<sub>2</sub>Cl<sub>2</sub>, and the precipitate that formed was dried in vacuo. Complex **1** was obtained as a green powder (isolated yield 68%). C<sub>44</sub>H<sub>62</sub>CuN<sub>2</sub>O<sub>4</sub>·H<sub>2</sub>O (746.5·H<sub>2</sub>O): calcd. C 69.12, H 8.44, N 3.66; found C 69.41, H 8.57, N 3.72. IR:

ν̄ = 1610 (C=N), 1577 (C=C), 1244 (C–O) cm<sup>−1</sup>. HRMS (ESI-TOF): calcd. for [M + H]<sup>+</sup> 746.4078; found 746.4070; error 1.18 ppm.

Complexes **2–6** were prepared similarly to **1**.

***N,N'*-(*o*-Phenylene)bis(4-decyloxysalicylideneiminato)copper(II) (**2**):** Green powder (isolated yield 57%). C<sub>40</sub>H<sub>54</sub>CuN<sub>2</sub>O<sub>4</sub>·2H<sub>2</sub>O (690.4·2H<sub>2</sub>O): calcd. C 66.13, H 8.05, N 3.86; found C 65.87, H 8.07, N 3.51. IR: ν̄ = 1606 (C=N), 1578 (C=C), 1244 (C–O) cm<sup>−1</sup>. HRMS (ESI-TOF): calcd. for [M + H]<sup>+</sup> 690.3452; found 690.3462; error −1.45 ppm.

***N,N'*-(*o*-Phenylene)bis(4-octyloxysalicylideneiminato)copper(II) (**3**):** Green powder (isolated yield 73%). C<sub>36</sub>H<sub>46</sub>CuN<sub>2</sub>O<sub>4</sub>·2H<sub>2</sub>O (634.3·2H<sub>2</sub>O): calcd. C 64.50, H 7.52, N 4.18; found C 65.06, H 7.61, N 3.66. IR: ν̄ = 1604 (C=N), 1578 (C=C), 1239 (C–O) cm<sup>−1</sup>. HRMS (ESI-TOF): calcd. for [M + H]<sup>+</sup> 634.2826; found 634.2821; error 0.81 ppm.

***N,N'*-(*o*-Phenylene)bis(4-dodecyloxysalicylideneiminato)nickel(II) (**4**):** Orange powder (isolated yield 57%). Analytical data for C<sub>44</sub>H<sub>62</sub>N<sub>2</sub>NiO<sub>4</sub>: <sup>1</sup>H NMR (200 MHz, CDCl<sub>3</sub>, 25 °C, TMS): δ = 0.88 (t, <sup>3</sup>J<sub>H,H</sub> = 6.6 Hz, 6 H, CH<sub>3</sub>), 1.27 (s, 36 H, CH<sub>2</sub>), 1.70–1.85 (m, 4 H, CH<sub>2</sub>), 3.95 (t, <sup>3</sup>J<sub>H,H</sub> = 6.5 Hz, 4 H, OCH<sub>2</sub>), 6.31 (dd, *J*<sub>H,H</sub> = 2.4 Hz, <sup>3</sup>J<sub>H,H</sub> = 8.8 Hz, 2 H, Ar-H), 6.61 (d, <sup>3</sup>J<sub>H,H</sub> = 2.0 Hz, 2 H, Ar-H), 7.13–7.21 (m, 4 H, Ar-H), 7.59–7.66 (m, 2 H, Ar-H), 8.06 (s, 2 H, HC=N) ppm. C<sub>44</sub>H<sub>62</sub>N<sub>2</sub>NiO<sub>4</sub>·H<sub>2</sub>O (741.7·H<sub>2</sub>O): calcd. C 69.56, H 8.49, N 3.69; found C 69.76, H 8.65, N 3.47. IR: ν̄ = 1604 (C=N), 1575 (C=C), 1252 (C–O) cm<sup>−1</sup>. HRMS (ESI-TOF): calcd. for [M + H]<sup>+</sup> 741.4136; found 741.4147; error −1.56 ppm.

***N,N'*-(*o*-Phenylene)bis(4-decyloxysalicylideneiminato)nickel(II) (**5**):** Reddish-orange powder (isolated yield 48%). Analytical data for C<sub>40</sub>H<sub>54</sub>N<sub>2</sub>NiO<sub>4</sub>: <sup>1</sup>H NMR (200 MHz, CDCl<sub>3</sub>, 25 °C, TMS): δ = 0.89 (t, <sup>3</sup>J<sub>H,H</sub> = 6.9 Hz, 6 H, CH<sub>3</sub>), 1.28 (s, 32 H, CH<sub>2</sub>), 1.71–1.85 (m, 4 H, CH<sub>2</sub>), 3.95 (t, <sup>3</sup>J<sub>H,H</sub> = 6.6 Hz, 4 H, OCH<sub>2</sub>), 6.30 (dd, *J*<sub>H,H</sub> = 2.3 Hz, <sup>3</sup>J<sub>H,H</sub> = 8.8 Hz, 2 H, Ar-H), 6.60 (d, <sup>3</sup>J<sub>H,H</sub> = 2.0 Hz, 2 H, Ar-H), 7.13–7.19 (m, 4 H, Ar-H), 7.58–7.67 (m, 2 H, Ar-H), 8.04 (s, 2 H, HC=N) ppm. C<sub>40</sub>H<sub>54</sub>N<sub>2</sub>NiO<sub>4</sub>·H<sub>2</sub>O (685.6·H<sub>2</sub>O): calcd. C 68.28, H 8.02, N 3.98; found C 68.65, H 7.95, N 3.71. IR: ν̄ = 1603 (C=N), 1575 (C=C), 1250 (C–O) cm<sup>−1</sup>. HRMS (ESI-TOF): calcd. for [M + H]<sup>+</sup> 685.3510; found 685.3518; error −1.18 ppm.

***N,N'*-(*o*-Phenylene)bis(4-octyloxysalicylideneiminato)nickel(II) (**6**):** Orange powder (isolated yield 37%). Analytical data for C<sub>36</sub>H<sub>46</sub>N<sub>2</sub>NiO<sub>4</sub>: <sup>1</sup>H NMR (200 MHz, CDCl<sub>3</sub>, 25 °C, TMS): δ = 0.90 (t, <sup>3</sup>J<sub>H,H</sub> = 6.4 Hz, 6 H, CH<sub>3</sub>), 1.30 (s, 20 H, CH<sub>2</sub>), 1.71–1.85 (m, 4 H, CH<sub>2</sub>), 3.95 (t, <sup>3</sup>J<sub>H,H</sub> = 6.5 Hz, 4 H, OCH<sub>2</sub>), 6.28 (d, <sup>3</sup>J<sub>H,H</sub> = 8.6 Hz, 2 H, Ar-H), 6.59 (s, 2 H, Ar-H), 7.11–7.16 (m, 4 H, Ar-H), 7.59–7.64 (m, 2 H, Ar-H), 8.00 (s, 2 H, HC=N) ppm. C<sub>36</sub>H<sub>46</sub>N<sub>2</sub>NiO<sub>4</sub>·H<sub>2</sub>O (629.5·H<sub>2</sub>O): calcd. C 66.78, H 7.47, N 4.33; found C 66.33, H 7.10, N 4.05. IR: ν̄ = 1602 (C=N), 1574 (C=C), 1249 (C–O) cm<sup>−1</sup>. HRMS (ESI-TOF): calcd. for [M + H]<sup>+</sup> 629.2884; found 629.2876; error 1.30 ppm.

In a typical procedure for Co<sup>II</sup> salophen complex synthesis, a solution of **D** (1.000 g, 1.46 mmol) in CH<sub>2</sub>Cl<sub>2</sub> (5 mL) was added to a warm solution of Co(OOCCH<sub>3</sub>)<sub>2</sub>·4H<sub>2</sub>O (0.482 g, 1.94 mmol) in MeOH (10 mL). A brown suspension immediately formed and was stirred for 4 h. The suspension was filtered, and the powder obtained was washed with MeOH. After drying in vacuo, the product was obtained as a dark brown powder.

***N,N'*-(*o*-Phenylene)bis(4-dodecyloxysalicylideneiminato)cobalt(II) (**7**):** Isolated yield 51%. C<sub>44</sub>H<sub>62</sub>CoN<sub>2</sub>O<sub>4</sub>·H<sub>2</sub>O (741.9·H<sub>2</sub>O): calcd. C 69.54, H 8.49, N 3.69; found C 69.58, H 8.79, N 3.39. IR: ν̄ = 1606 (C=N), 1578 (C=C), 1240 (C–O) cm<sup>−1</sup>. HRMS (ESI-TOF): calcd. for [M]<sup>+</sup> 741.4036; found 741.4037; error −0.10 ppm.

***N,N'*-(*o*-Phenylene)bis(4-decyloxysalicylideneiminato)cobalt(II) (8):** Isolated yield 68%.  $C_{40}H_{54}CoN_2O_4 \cdot 2H_2O$  (685.8·2H<sub>2</sub>O): calcd. C 66.56, H 8.10, N 3.88; found C 66.43, H 8.10, N 3.72. IR:  $\tilde{\nu}$  = 1604 (C=N), 1577 (C=C), 1241 (C–O) cm<sup>−1</sup>. HRMS (ESI-TOF): calcd. for [M]<sup>+</sup> 685.3410; found 685.3400; error 1.41 ppm.

***N,N'*-(*o*-Phenylene)bis(4-octyloxysalicylideneiminato)cobalt(II) (9):** Isolated yield 41%.  $C_{36}H_{46}CoN_2O_4 \cdot H_2O$  (629.7·H<sub>2</sub>O): C 66.76, H 7.47, N 4.32; found C 66.98, H 7.53, N 3.90. IR:  $\tilde{\nu}$  = 1603 (C=N), 1579 (C=C), 1239 (C–O) cm<sup>−1</sup>. HRMS (ESI-TOF): calcd. for [M]<sup>+</sup> 629.2790; found 629.2775; error 2.32 ppm.

**Supporting Information** (see footnote on the first page of this article): STM images of complexes **5**, **6**, **8** and **9**.

## Acknowledgments

We gratefully acknowledge the financial support of the Magnus Ehrnrooth Foundation, TEKES and Academy of Finland as well as the “Sonderforschungsbereich” SFB 569 (“Hierarchic structure formation and function of organic-inorganic nano systems”) of the German Science Foundation DFG.

- [1] a) A. Ulman, S. D. Evans, Y. Shnidman, R. Sharma, J. E. Eilers, J. C. Chang, *J. Am. Chem. Soc.* **1991**, *113*, 1499–1506; b) A. Ulman, J. F. Kang, Y. Shnidman, S. Liao, R. Jordan, G.-Y. Choi, J. Zaccaro, A. S. Myerson, M. Rafailovich, J. Sokolov, C. Fleischer, *Rev. Mol. Biotechnol.* **2000**, *74*, 175–188; c) G. C. Herdt, D. R. Jung, A. W. Czanderna, *Prog. Surf. Sci.* **1995**, *50*, 103–129.
- [2] a) R. Izumi, K. Hayama, K. Hayashi, K. Toko, *Chem. Sens.* **2004**, *20*, 50–51; b) J. Ladd, C. Boozer, Q. Yu, S. Chen, J. Homola, S. Jiang, *Langmuir* **2004**, *20*, 8090–8095; c) S. Huan, G. Shen, R. Yu, *Electroanalysis* **2004**, *16*, 1019–1023; d) F. Maya, A. K. Flatt, M. P. Stewart, D. E. Shen, J. M. Tour, *Chem. Mater.* **2004**, *16*, 2987–2997.
- [3] S. Flink, B. A. Boukamp, A. van den Berg, F. C. J. M. van Veghel, D. N. Reinhoudt, *J. Am. Chem. Soc.* **1998**, *120*, 4652–4657.
- [4] G. A. Somorjai, *Chemistry in Two Dimensions: Surfaces*, Cornell University Press, Ithaca NY, **1981**.
- [5] a) C. M. Whelan, M. Kinsella, H. M. Ho, K. Maex, *J. Electrochem. Soc.* **2004**, *151*, B33–B38; b) Z. Quan, S. Chen, X. Cui, Y. Li, *Corrosion (Houston, TX, U. S.)* **2002**, *58*, 248–256; c) S. Ramachandran, B.-L. Tsai, M. Blanco, H. Chen, Y. Tang, W. A. Goddard III, *Langmuir* **1996**, *12*, 6419–6428.
- [6] Q. Zhang, L. A. Archer, *J. Phys. Chem. B* **2003**, *107*, 13123–13132.
- [7] a) M. K. Chaudhury, G. M. Whitesides, *Science* **1992**, *255*, 1230–1232; b) R. K. Smith, P. A. Lewis, P. S. Weiss, *Prog. Surf. Sci.* **2004**, *75*, 1–68.
- [8] a) C. D. Bain, G. M. Whitesides, *Angew. Chem. Int. Ed. Engl.* **1989**, *28*, 506–512; b) G. M. Whitesides, P. E. Laibinis, *Langmuir* **1990**, *6*, 87–96; c) P. E. Laibinis, R. G. Nuzzo, G. M. Whitesides, *J. Phys. Chem.* **1992**, *96*, 5097–5105.
- [9] a) T. Ikeda, M. Asakawa, M. Goto, K. Miyake, T. Ishida, T. Shimizu, *Langmuir* **2004**, *20*, 5454–5459; b) P. Qian, H. Nanjo, N. Sanada, T. Yokoyama, T. M. Suzuki, *Chem. Lett.* **2000**, 1118–1119; c) I. Sakata, K. Miyamura, *Chem. Commun.* **2003**, 156–157; d) X. Qiu, C. Wang, Q. Zeng, B. Xu, S. Yin, H. Wang, S. Xu, C. Bai, *J. Am. Chem. Soc.* **2000**, *122*, 5550–5556; e) T. Ohshiro, T. Ito, P. Bühlmann, Y. Umezawa, *Anal. Chem.* **2001**, *73*, 878–883; f) P. Zell, F. Mögele, U. Ziener, B. Rieger, *Chem. Eur. J.* **2006**, *12*, 3847–3857; g) S. De Feyter, M. M. S. Abdel-Mottaleb, N. Schuurmans, B. J. V. Verkuijl, J. H. van Esch, B. L. Feringa, F. C. De Schryver, *Chem. Eur. J.* **2004**, *10*, 1124–1132.
- [10] D. Yin, S. Horiuchi, M. Morita, A. Takahara, *Langmuir* **2005**, *21*, 9352–9358.
- [11] a) M. S. Alam, S. Strömsdörfer, V. Dremov, P. Müller, J. Kortus, M. Ruben, J.-M. Lehn, *Angew. Chem. Int. Ed.* **2005**, *44*, 7896–7900; b) A. Semenov, J. P. Spatz, M. Möller, J.-M. Lehn, B. Sell, D. Schubert, C. H. Weidl, U. S. Schubert, *Angew. Chem. Int. Ed.* **1999**, *38*, 2547–2550; c) N. Lin, S. Stepanow, F. Vidal, K. Kern, M. S. Alam, S. Strömsdörfer, V. Dremov, P. Müller, A. Landa, M. Ruben, *Dalton Trans.* **2006**, 2794–2800; d) U. Ziener, J.-M. Lehn, A. Mourran, M. Möller, *Chem. Eur. J.* **2002**, *8*, 951–957.
- [12] A. Mourran, U. Ziener, M. Möller, E. Breuning, M. Ohkita, J.-M. Lehn, *Eur. J. Inorg. Chem.* **2005**, 2641–2647.
- [13] a) G. S. Hanan, D. Volkmer, U. S. Schubert, J.-M. Lehn, G. Baum, D. Fenske, *Angew. Chem. Int. Ed. Engl.* **1997**, *36*, 1842–1844; b) M. Ruben, E. Breuning, J.-P. Gisselbrecht, J.-M. Lehn, *Angew. Chem. Int. Ed.* **2000**, *39*, 4139–4142; c) E. Breuning, M. Ruben, J.-M. Lehn, F. Renz, Y. Garcia, V. Ksenofontov, P. Gütllich, E. Wegelius, K. Rissanen, *Angew. Chem. Int. Ed.* **2000**, *39*, 2504–2507; d) O. Waldmann, J. Hassmann, P. Müller, G. S. Hanan, D. Volkmer, U. S. Schubert, J.-M. Lehn, *Phys. Rev. Lett.* **1997**, *78*, 3390–3393; e) M. Ruben, J.-M. Lehn, G. Vaughan, *Chem. Commun.* **2003**, 1338–1339; f) M. Ruben, E. Breuning, J.-M. Lehn, V. Ksenofontov, F. Renz, P. Gütllich, G. B. M. Vaughan, *Chem. Eur. J.* **2003**, *9*, 4422–4429; g) M. Ruben, U. Ziener, J.-M. Lehn, V. Ksenofontov, P. Gütllich, G. B. M. Vaughan, *Chem. Eur. J.* **2005**, *11*, 94–100.
- [14] B. A. Hermann, L. J. Scherer, C. E. Housecroft, E. C. Constable, *Adv. Funct. Mater.* **2006**, *16*, 221–235.
- [15] a) M. Surin, P. Samorì, A. Jouaiti, N. Kyritsakan, M. W. Hosseini, *Angew. Chem. Int. Ed.* **2007**, *46*, 245–249; b) L. Pirondini, A. G. Stendardo, S. Geremia, M. Campagnolo, P. Samorì, J. P. Rabe, R. Fokkens, E. Dalcanele, *Angew. Chem. Int. Ed.* **2003**, *42*, 1384–1387; c) A. P. Seitsonen, M. Lingenfelder, H. Spillmann, A. Dmitriev, S. Stepanow, N. Lin, K. Kern, J. V. Barth, *J. Am. Chem. Soc.* **2006**, *128*, 5634–5635; d) S. Clair, S. Pons, S. Fabris, S. Baroni, H. Brune, K. Kern, J. V. Barth, *J. Phys. Chem. B* **2006**, *110*, 5627–5632; e) T. Classen, G. Fratesi, G. Costantini, S. Fabris, F. L. Stadler, C. Kim, S. de Gironcoli, S. Baroni, K. Kern, *Angew. Chem. Int. Ed.* **2005**, *44*, 6142–6145; f) S. Clair, S. Pons, H. Brune, K. Kern, J. V. Barth, *Angew. Chem. Int. Ed.* **2005**, *44*, 7294–7297; g) S. Stepanow, N. Lin, J. V. Barth, K. Kern, *J. Phys. Chem. B* **2006**, *110*, 23472–23477; h) A. Dmitriev, H. Spillmann, N. Lin, J. V. Barth, K. Kern, *Angew. Chem. Int. Ed.* **2003**, *42*, 2670–2673; i) H. Spillmann, A. Dmitriev, N. Lin, P. Messina, J. V. Barth, K. Kern, *J. Am. Chem. Soc.* **2003**, *125*, 10725–10725; j) S. Stepanow, N. Lin, J. V. Barth, K. Kern, *Chem. Commun.* **2006**, 2153–2155.
- [16] Though solvent molecules can be coordinated to the axial positions of the metal centres in the 2D assemblies of the studied complexes, this is believed to have only a minor influence on the surface patterns created. Also, attempts at imaging the corresponding salen complexes and the salophen complexes with hexyloxy side chains were not successful. We therefore propose that in particular, salen complexes with C<sub>6</sub>–C<sub>12</sub> chains, salophen complexes with C<sub>6</sub> chains and salophen ligands with alkyl chains shorter than 12 carbons are too mobile on HOPG for successful STM imaging. It has been previously reported that even if the molecules are easily adsorbed on the surface, high-resolution images may be difficult to obtain because of the mobility of the molecules within the basal plane. Also, the scanning tip may introduce a perturbation which would interfere with the imaging. [see ref.<sup>[9a,9c,9d]</sup> and D. M. Cyr, B. Venkataraman, G. W. Flynn, *Chem. Mater.* **1996**, *8*, 1600–1615].
- [17] C. L. Claypool, F. Faglioni, W. A. Goddard III, H. B. Gray, N. S. Lewis, R. A. Marcus, *J. Phys. Chem. B* **1997**, *101*, 5978–5995.
- [18] a) G. R. Desiraju, *Chem. Commun.* **2005**, 2995–3001; b) C. Meier, U. Ziener, K. Landfester, P. Wehrich, *J. Phys. Chem. B* **2005**, *109*, 21015–21027.
- [19] a) J. H. Chou, M. E. Kosal, H. S. Nalwa, N. A. Rakow, K. S. Suslick, *The Porphyrin Handbook*, Academic Press: New York,



- 2000, 6, 43–131; b) A. Zlatkin, S. Yudin, J. Simon, M. Hanack, H. Lehmann, *Adv. Mater. Opt. Electron.* **1995**, 5, 259–263; c) L. Scudiero, D. E. Barlow, K. W. Hipps, *J. Phys. Chem. B* **2002**, 106, 996–1003.
- [20] K. G. Nath, O. Ivasenko, J. A. Miwa, H. Dang, J. D. Wuest, A. Nanci, D. F. Perepichka, F. Rosei, *J. Am. Chem. Soc.* **2006**, 128, 4212–4213.
- [21] Cu complexes with C<sub>10</sub> and C<sub>12</sub> alkyl chains formed another new 2D pattern on the liquid–graphite interface. The only difference in these patterns is the periodicity in one of the directions which varies predictably with the alkyl chain length. Even though a high-resolution STM image was obtained for complex **2**, the resolution was still not high enough to allow us to propose a proper structural model.
- [22] K. Binnemans, Y. G. Galyametdinov, R. Van Deun, D. W. Bruce, S. R. Collinson, A. P. Polishchuk, I. Bikchantaev, W. Haase, A. V. Prosvirin, L. Tinchurina, I. Litvinov, A. Gubajdullin, A. Rakhmatullin, K. Uytterhoeven, L. van Meervelt, *J. Am. Chem. Soc.* **2000**, 122, 4335–4344.

Received: February 2, 2007

Published Online: July 6, 2007